Bol. Soc. Paran. Mat.
©SPM – E-ISSN-2175-1188
SPM: www.spm.uem.br/bspm

(3s.) **v. 2025 (43)** : 1–13.
ISSN-0037-8712
doi:10.5269/bspm.77253

Hybrid Spectral-Runge-Kutta Method for Solving Nonlinear Stochastic Differential Equations

Mohammed I. Abdulkareem and Ayad R. Khudair*

ABSTRACT: This paper concerns solving nonlinear stochastic differential equations (SDEs) by enhancing a novel method. There are two primary steps towards constructing this method. The core idea of the first step involves approximating each Brownian sample path over the given time horizon utilising Chebyshev polynomials. The second task is solved by using the Runge-Kutta method. In fact, the procedure in step one allowed us to utilise the classical Runge-Kutta method for stochastic differential equations without necessitating any alterations to their original formulations. Comprehensive numerical experiments on various test problems reveal that the proposed hybrid method achieves significantly lower average absolute errors, calculated over 10,000 sample paths, compared to five established techniques (Euler-Maruyama, Milstein, Stochastic Runge-Kutta (Platen), block-pulse, and hat-function methods), while maintaining a similar computational cost. In fact, the convergence and stability of this hybrid method are inhibited by the original Chebyshev approximation and the classical Runge-Kutta method. Also, the hybrid method provides a flexible and effective instrument for the precise simulation of nonlinear stochastic differential equations.

Key Words: Nonlinear stochastic differential equations, First-kind Chebyshev polynomials, direct collocation technique, Runge-Kutta method.

Contents

1. Introduction

Applied mathematics offers essential tools and methodologies for converting real-world phenomena into accurate mathematical models [30,17,1,15], with stochastic differential equations (SDEs) have become essential instruments for modelling systems affected by uncertainty and random variations, with applications across telecommunications, economics, finance, biology, ecology, and various other scientific fields [31,41,2,23,18,12]. Additionally, fractional differential equations, by incorporating nonlocal, memory-dependent effects, surpass integer-order models in accurately depicting anomalous transport, viscoelasticity, and intricate biological processes [28,16,29,25,30]. Also, fractional stochastic differential equations incorporate randomness to model noise-driven systems characterised by long-range temporal correlations and heavy-tailed variability across disciplines such as finance, climate science, and biophysics SDEs fundamentally expand ordinary differential equations (ODEs) by integrating stochastic perturbations, thus encapsulating the intrinsic randomness of real-world dynamics [6,21,20,19]. In contrast to ordinary differential equations, most stochastic differential equations do not permit closed-form solutions.

Unfortunately, analytic solutions are typically inaccessible in general, except in certain exceptional instances (e.g., linear systems with constant coefficients), owing to the intrinsic randomness of the driving noise and possible nonlinearities in the drift and diffusion components. Thus, numerical approximation

* Corresponding author.
2010 *Mathematics Subject Classification:* 60H35, 65C30, 65C20, 65L06, and 65M70.
Submitted June 08, 2025. Published December 05, 2025

methods are crucial as they facilitate the simulation of sample trajectories and the estimation of statistical measures, including moments, hitting time distributions, and density functions. Indeed, various numerical methods has been developed to address the challenges presented by SDEs. Prominent among these are the truncated Euler-Maruyama method [10], several Runge-Kutta schemes [46], the delta function method [32], and semi-implicit Euler methods [9]. The numerical methodological framework is enhanced by various supplementary approaches, including meshless methods [35], operational matrix techniques [34], finite difference methods [8], fourth order hat function [37,39,27,26,38] and wavelet-based computational algorithms [45]. The application of polynomial basis functions, including shifted Legendre polynomials [24] and Euler polynomials [36], has proven highly effective in tackling the inherent nonlinearity and complexity of these equations.

Conversely, owing to the ability to directly represent nonlinear terms in the Chebyshev basis, the formulation of discrete algebraic systems and the associated computational costs are pertinent to low-order schemes. Spectral methods utilising Chebyshev polynomial approximations demonstrate remarkable efficiency and accuracy in the numerical resolution of various nonlinear ODEs. Employing a collocation framework at the Chebyshev-Gauss-Lobatto nodes, one constructs high-order differentiation matrices distinguished by exponential convergence for smooth solutions and proficient management of boundary layers, making them particularly suitable for stiff and nonlinear problems [47,42]. Motivated by these achievements, recent research has expanded Chebyshev spectral methods to SDEs through the introduction of modified operational matrices that discretise Itâ integrals within the Chebyshev domain. Barikbin et al. [4] proposed an iterative method employing shifted Chebyshev polynomials for the numerical resolution of SDEs by converting the SDE into its corresponding Itô Volterra integral representation. They discretised both the deterministic and stochastic integrals using Chebyshev operational matrices, subsequently transforming the resulting integral equations into a coupled system of nonlinear algebraic equations.

In fact, the numerical method is still the best way toward solving nonlinear SDEs. Meanwhile, it faces major obstacles pertaining to convergence, accuracy, and the balance between accuracy and robustness. Classical time-stepping methods, including the Euler-Maruyama [13], Milstein methods [7], and Stochastic Runge-Kutta [22], are easy to implement and maintain stability under minimal smoothness conditions; however, they typically provide only low-order convergence. On the other hand, the classical deterministic fourth-order Runge-Kutta (RK4) can not be applied directly due to the SDE involving non-differentiable (Brownian) increments. Furthermore, due to it neither respecting the Itô correction nor attaining the correct strong or weak order for stochastic integrals. The main objective motivation for this work is to introduce a novel hybrid method to address these issues. This hybrid method is constructed from combining the Chebyshev spectral approximation method together with the classical deterministic RK4. This hybrid method will benefit from the exponential convergence of the Chebyshev spectral approximation method and the fourth-order convergence of RK4.

The outstanding sections of this paper are prepared as follows: In Section 2, we explore the formulation of stochastic differential equations and the vital information on Brownian motion. In Section 3, we construct a hybrid method by using the Chebyshev spectral approximation method to precisely approximate the sample paths of Brownian motion over a finite interval. Then, we solve the resulting differential equations by the deterministic RK4. Section 4 provides a several test problem for numerical experiments that illustrate the applicability, precision, and computational efficiency of the proposed method on representative test cases. Section 5 concludes with a summary of our principal results and delineates potential avenues for future research.

2. Preliminary

This study concentrates on the numerical resolution of nonlinear SDEs represented by the following general form:

$$\begin{aligned} dY_t &= \phi(t, Y_t)dt + \varphi(t, Y_t)dB(t), \quad t \in [0, T], \\ Y_0 &= Y0. \end{aligned} \tag{2.1}$$

where $\phi(t, Y_t)$ represent the drift coefficient and $\varphi(t, Y_t)$ the diffusion coefficient that are are smooth functions on $\mathbb{R}$. Also, $dB(t) = W(t)dt$ represents the formally differential of a standard Brownian motion

$B(t)$) [40,14]. Moreover, any solution of the stochastic differential equation is also a solution of the subsequent Volterra integral equation:

$$Y_t = Y0 + \int_0^t \phi(s, Y_s)ds + \int_0^t \varphi(s, Y_s)dB(s), \quad t \in [0, T]. \tag{2.2}$$

In the reminding section, we outline the essential components of our study: the definition and statistical properties of Brownian motion, its simulation methodology; the core principles and techniques of stochastic calculus; and the pivotal theory of orthogonal Chebyshev polynomials that underpins the numerical analyses discussed in this work.

Definition 2.1 [41] Let $(\Omega, \mathcal{F}, P)$ denote a probability space, and let I represent a totally ordered index set, typically $\mathbb{R}$ or a subset thereof. For every $i \in I$, let $\mathcal{F}_i$ denote a sub-σ-algebra of $\mathcal{F}$. The collection $\{\mathcal{F}_i\}_{i\in I}$ constitutes a filtration if for any indices i and j where $i < j$, it follows that $\mathcal{F}_i \subseteq \mathcal{F}_j$. When this condition is met, the probability space $(\Omega, \mathcal{F}, P)$ is designated as a filtered probability space.

Definition 2.2 [41] Standard Brownian motion, also known as the Wiener process, is a classification for a stochastic process $B(t)$ with continuous sample paths defined for $t \geq 0$, provided it meets the following criteria:

- *Initial Condition: The process commences at the origin, indicating that* $B(0) = 0$ *with high probability.*
- *Autonomous Increments: For any sequence of time points* $0 = t_0 < t_1 < \cdots < t_n$*, the increments* $B(t_{k+1}) - B(t_k)$ *are independent of one another.*
- *Stationary Increments: The distribution of the increment* $B(t + h) - B(t)$ *is independent of the particular time* t *and relies exclusively on the increment* h*.*
- *Gaussian Marginals: For all* $t \geq 0$*, the random variable* $B(t)$ *follows a normal distribution with a mean of 0 and a variance of 1, and its sample paths are continuous functions of time.*

Definition 2.3 *[44] Suppose* Y_t *represents a measurable stochastic process defined on the filtration* $\{\Im_t\}, \forall t \geq 0$*, such that*

$$\int_p^q Y_t dB(t) = \lim_{\ell\to\infty} \sum_{i=0}^{\ell-1} Y_{t_i} \left(B(t_{i+1}) - B(t_i)\right), \quad t_i = p + \frac{q-p}{\ell} i \ , \ \ i = 0, 1, \ldots, \ell \tag{2.3}$$

then integration in (2.3) is referred to as the Itâ integral of Y_t*. To rephrase,*

$$E\left[\left|\int_p^q Y_t dB - \sum_{i=0}^{\ell-1} Y_{t_i} \left(B(t_{i+1}) - B(t_i)\right)\right|^2\right] \to 0, \quad as \ \ \ell \to \infty.$$

3. Proposed Numerical Method

This section develops a novel numerical approach for nonlinear SDEs via the modification of Chebyshev methods. The enhancement relies on partitioning the overall time frame, [0, T], into $P = NM$, such that:

$$h = \Delta t = \frac{T}{P}, \quad \text{where } N \text{ and } M \text{ are integer positive constants, and } \quad T_j = j\,\Delta t.$$

This yields $P + 1$ time-points $t_0, t_1, \ldots, t_P$.

The first step toward solving SDEs numerically is generating Brownian motion over time horizon $[0, T]$ as follows:

- For each subinterval $[t_{k-1}, t_k]$, define Brownian increments as independent normal random variables as follows:

$$\Delta B_k \ \sim \ \mathcal{N}(0, \Delta t), \quad k = 1, 2, \ldots, P.$$

- For k = 1,2,..., P, we set
$$B_k = B_{k-1} + \Delta B_k,$$
where $B_0 = 0$.
- The sequence $\{(t_k, B_k)\}_{k=0}^{P}$ represent a discrete approximation of a Brownian path on the interval $[0, T]$.

3.1. Approximation of Brownian motion utilising Chebyshev polynomials

Consider the sample paths of Brownian motion on the interval $[0, T]$ which generated by sequence of points $\{(t_k, B_k)\}_{k=0}^{P}$. The main idea of this subsection is design a piecewise function, $\Xi(t)$, that coincides with all $MN + 1$ points of the sample paths of Brownian motion as follows:

$$\Xi(t) = \begin{cases} \Xi_0(t), & t \in [0, Mh], \\ \Xi_1(t), & t \in [Mh, 2Mh], \\ \vdots & \vdots \\ \Xi_{N-2}(t), & t \in [(N-2)Mh, (N-1)Mh], \\ \Xi_{N-1}(t), & t \in [(N-1)Mh, Ph]. \end{cases} \tag{3.1}$$

However, we utilise the M Chebyshev polynomial for constructing each $\Xi_k(t)$ within the subdomain $[kMh, (k+1)Mh]$. For all $k = 0, 1, \ldots, N-1$ such that

$$\Xi_k(t) = \sum_{j=0}^{M} \beta_{j,k} T_j\left(\frac{2(t - khM)}{hM} - 1\right), \qquad k = 0, 1, \ldots, N-1. \tag{3.2}$$

We will now assign the value of $t = khM + ih$ in (3.2) for $i = 0, 1, \ldots, M$ and $k = 0, 1, \ldots, N-1$. This leads to the following expression:

$$\sum_{j=0}^{M} \beta_{j,k} T_j\left(\frac{2i}{M} - 1\right) = B(khM + ih), \quad i = 0, 1, \ldots, M, \quad k = 0, 1, \ldots, N-1, \tag{3.3}$$

which depiction can be articulated in matrix format as

$$AC_k = b_k, \qquad k = 0, 1, \ldots, N-1, \tag{3.4}$$

where

$$A = \begin{pmatrix} T_0(-1) & T_1(-1) & T_2(-1) & \cdots & T_M(-1) \\ T_0(\frac{2}{M} - 1) & T_1(\frac{2}{M} - 1) & T_2(\frac{2}{M} - 1) & \cdots & T_M(\frac{2}{M} - 1) \\ T_0(\frac{4}{M} - 1)) & T_1(\frac{4}{M} - 1) & T_2(\frac{4}{M} - 1)) & \cdots & T_M(\frac{4}{M} - 1)) \\ \vdots & \vdots & \vdots & \ddots & \vdots \\ T_0(1) & T_1(1) & T_2(1) & \cdots & T_M(1) \end{pmatrix},$$

$$C_k = \begin{pmatrix} \beta_{0,k} \\ \beta_{1,k} \\ \beta_{2,k} \\ \vdots \\ \beta_{M-1,k} \\ \beta_{M,i} \end{pmatrix}, \qquad b_k = \begin{pmatrix} B(khM) \\ B(khM + h) \\ B(khM + 2h) \\ \vdots \\ B(khM + (M-1)h) \\ B(khM + Mh) \end{pmatrix}.$$

It should be emphasised that the matrix A is a Vandermonde-type collocation matrix, thus $|A| = 2^{\frac{M(M-1)}{2}} \prod_{0 \le i < j \le M} (a_i - a_j)$ [5], due to $a_i = \frac{2i}{M} - 1$ being distinct for $i = 0, 1, \ldots, M$. Hence, the matrix A is invertible. It is easy to find all required constants $\beta_{j,k}$, $j = 0, 1, \ldots, M$, $k = 0, 1, \ldots, N-1$ via

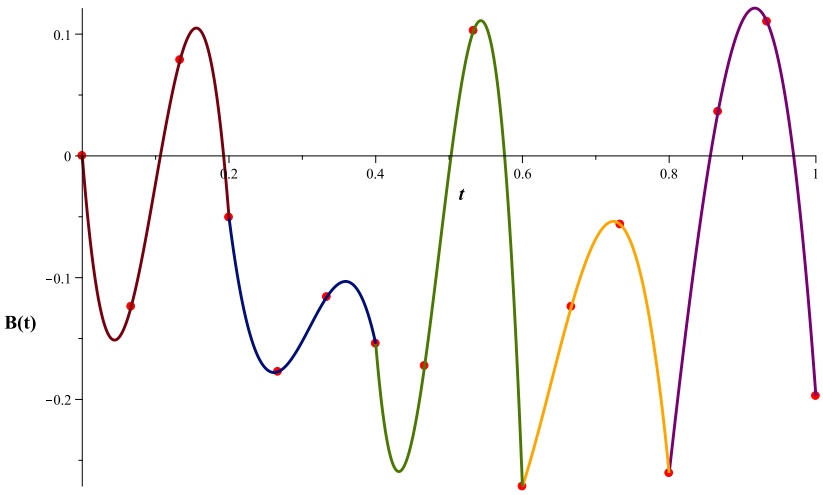

Figure 1: Approximate the Brownian motion via a piecewise function $\Xi(t)$ in (3.6).

compute $C_k = A^{-1}b_k, \quad k = 0, 1, \ldots, N-1$.

Now, we demonstrate the construction of the piecewise function match using the one sample path of Brownian motion at $NM + 1 = 16$ points, where $N = 5$ denotes the number of subdomains of $[0, 1]$ and $M = 3$. It is straightforward to ascertain that:

$$A = \begin{pmatrix} 1 & 1 & 1 & 1 \\ -1 & \frac{-1}{3} & \frac{1}{3} & 1 \\ 1 & \frac{-7}{9} & \frac{-7}{9} & 1 \\ -1 & \frac{23}{27} & \frac{-23}{27} & 1 \end{pmatrix}, \qquad A^{-1} = \begin{pmatrix} \frac{7}{32} & \frac{-23}{64} & \frac{9}{32} & \frac{-9}{64} \\ \frac{9}{32} & \frac{-27}{64} & \frac{-9}{32} & \frac{27}{64} \\ \frac{9}{32} & \frac{27}{64} & \frac{-9}{32} & \frac{-27}{64} \\ \frac{7}{32} & \frac{23}{64} & \frac{9}{32} & \frac{9}{64} \end{pmatrix}.$$

By adhering to the prior simulation procedure for Brownian motion, we generate the subsequent 16 points:

$$\begin{gathered}[0,0],[\tfrac{1}{15},-0.124],[\tfrac{2}{15},0.0787],[\tfrac{3}{15},-0.0505],[\tfrac{4}{15},-0.177],[\tfrac{5}{15},-0.116],[\tfrac{6}{15},-0.154],[\tfrac{7}{15},-0.172], \\ [\tfrac{8}{15},0.103],[\tfrac{9}{15},-0.271],[\tfrac{10}{15},-0.124],[\tfrac{11}{15},-0.0563],[\tfrac{12}{15},-0.261],[\tfrac{13}{15},0.0363],[\tfrac{14}{15},0.110],[1,-0.197]\end{gathered} \tag{3.5}$$

One can directly utilise (3.4) to calculate the unknown coefficient, $\beta_{j,k}$, in (3.3), and subsequently employ (3.1) to determine the ensuing piecewise function that matches the sample path point of Brownian motion in (3.5):

$$\Xi(t) = \begin{cases} -0.368 + 3.45t - 0.00308(10t-1)^2 - 0.370(10t-1)^3, & t \in [0, 0.2), \\ -0.482 + 1.11t + 0.0498(10t-3)^2 - 0.162(10t-3)^3, & t \in [0.2, 0.4), \\ -2.38 + 4.73t - 0.200(10t-5)^2 - 0.532(10t-5)^3, & t \in [0.4, 0.6), \\ -0.860 + 1.13t - 0.198(10t-7)^2 - 0.108(10t-7)^3, & t \in [0.6, 0.8), \\ -0.977 + 1.21t - 0.340(10t-9)^2 - 0.0892(10t-9)^3, & t \in [0.8, 1]. \end{cases} \tag{3.6}$$

Figure (1) elucidates the match between the one sample path points of the Brownian motion (3.5), indicated by the red points, and the coloured piecewise functions that represent $\Xi(t)$ in (3.6).

3.2. Applying classical fourth-order Runge-Kutta

Based on the fact that the SDE involves non-differentiable (Brownian) increments, the classical deterministic fourth-order Runge-Kutta (RK4) is not able to apply directly. Due to it neither respecting the

Itô correction nor attaining the correct strong or weak order for stochastic integrals. However, there are some methods used to solve nonlinear SDEs, including Euler-Maruyama (strong order 0.5) [13], Milstein's method (strong order 1.0) [7], and Stochastic Runge-Kutta methods (Platen's method of strong order 1.5 or 2.0) [22]. These methods specific for SDEs include extra terms (Itô-corrections, multiple stochastic increments) that the classical RK4 omits.

However, the approximation of sample paths of Brownian motion on the interval $[0,T]$ utilising Chebyshev polynomials as in (3.1) gives us an advantage to overcome the difficulty of dealing with Brownian motion. Due to $\Xi(t)$, which is defined in (3.1) is a differentiable function over each subinterval $[kMh,(k+1)Mh]$, for all $k=0,1,\ldots,N-1$. This motivated us to apply the classical deterministic RK4 for each subinterval $[kMh,(k+1)Mh]$ directly.

$$\begin{aligned} dy(t) &= \phi(t,y(t))dt + \varphi(t,y(t))\,\Xi'_0(t)\,dt, \quad t\in[0,Mh],\\ y(0) &= Y0,\\ dy(t) &= \phi(t,y(t))dt + \varphi(t,y(t))\,\Xi'_k(t)\,dt, \quad t\in[kMh,(k+1)Mh],\\ y(kMh) &= y((k-1)Mh), \qquad\qquad \forall k=1,2,...,N-1, \end{aligned} \tag{3.7}$$

where $y(hk)$ is approximate to stochastic process Y_t at $t=hk$ for each $k=0,1,...,NM$. It is easy to see that for fixed sample paths of Brownian motion on the interval $[0,T]$, the differential equations (3.7) are merely ordinary differential equations.

Now, we assume $h_1=\frac{h}{S}$ for a given positive integer S, and then set $t_{k,n}=khM+nh_1$ and $y_{k,n}=y(t_{k,n})$. Hence, the RK4 method can be formulate as follows:

$$y_{k,n+1}=y_{k,n}+\frac{h_1}{6}(K_{k,1}+2K_{k,2}+2K_{k,3}+K_{k,4}), \quad n=0,1,...,SM,\ \ k=0,1,...,N-1, \tag{3.8}$$

where

$$\begin{aligned} K_{k,1} &= \phi(t_n,y(t_n))+\varphi(t_n,y(t_n))\,\Xi'_k(t_n)\\ K_{k,2} &= \phi(t_n+\frac{h_1}{2},y(t_n+\frac{h_1K_{k,1}}{2}))+\varphi(t_n+\frac{h_1}{2},y(t_n+\frac{h_1K_{k,1}}{2}))\,\Xi'_k(t_n+\frac{h_1}{2})\\ K_{k,3} &= \phi(t_n+\frac{h_1}{2},y(t_n+\frac{h_1K_{k,2}}{2}))+\varphi(t_n+\frac{h_1}{2},y(t_n+\frac{h_1K_{k,2}}{2}))\,\Xi'_k(t_n+\frac{h_1}{2})\\ K_{k,4} &= \phi(t_n+h_1,y(t_n+h_1K_{k,3}))+\varphi(t_n+h_1,y(t_n+h_1K_{k,3}))\,\Xi'_k(t_n+h_1), \end{aligned} \tag{3.9}$$

with $y_{0,0}=Y0$ and $y_{k,0}=y((k-1)Mh)$ for $k=1,2,...,N-1$.

Since the proposed hybrid method is constructed from two well-known convergent methods, we need not re-derive its convergence. In fact, the Chebyshev polynomial approximation of the Brownian motion path established spectral exponential convergence rates under mild regularity assumptions, as well as the classical RK4 method, which guarantees fourth-order accuracy and zero stability for the resulting deterministic system. By standard results, a stable, consistent composition of these two methods inherits the minimum of their individual convergence orders. Moreover, the global error can be decomposed additively into the Chebyshev interpolation error and the RK4 discretisation error, both of which are already quantified in the literature, so no new convergence proof is required beyond citing those existing bounds.

4. Illustrated Examples

In this section, we present several numerical examples to illustrate the efficiency, accuracy, and practical applicability of the proposed hybrid spectral time-stepping method. All calculations were conducted on a personal laptop featuring 11th Gen Intel(R) Core(TM) i9-11900H @ 2.50 GHz. In our experiments, we utilised 10,000 sample paths of Brownian motion, produced with high-resolution time discretisation. To rigorously evaluate the advantages of our technique, we have carried out a direct head-to-head comparison with five numerical methods, including Euler-Maruyama, Milstein, Stochastic Runge-Kutta (Platen), block-pulse, and hat-function methods. To evaluate the efficacy of our method, we juxtapose the approximate numerical solution with the exact solution across 10,000 Brownian motion sample paths;

at each fixed time point, we calculate the sample average and ascertain the absolute average error using the subsequent formula:

$$e(t) = \sum_{i=1}^{10000} |Y_t^i - \tilde{Y}_t^i|,$$

where Y_t^i and $\tilde{Y}_t^i$ are the exact stochastic process and the approximate stochastic process at the i^{th} sample path of Brownian motion, respectively.

Example 4.1 Consider the following linear SDE that delineates the canonical model for stock price dynamics in mathematical finance, commonly known as geometric Brownian motion [40]:

$$dY_t = \frac{2}{\alpha} Y_s + \frac{1}{\alpha} Y_s \, dB(s), \quad \forall t \in [0, 1], \tag{4.1}$$

with $Y_0 = \beta$. Here the exact stochastic process is

$$Y_t \;=\; \beta \exp\!\left(\left(\tfrac{2}{\alpha} - \tfrac{1}{2\alpha^2} \right) t \;+\; \tfrac{1}{\alpha} B(t) \right). \tag{4.2}$$

Table 1: The average absolute error calculated across 10,000 sample paths for Example 4.1.

Time	Present Method $P = 8$	Euler-Maruyama $N = 32$ [13]	Milstein $N = 32$ [7]	Platen $N = 32$ [22]	Block Pulse $N = 8$ [3]	Hat Functions $N = 8$ [11]
0.125	1.116E-06	6.607E-05	6.598E-05	6.618E-05	2.265E-06	2.055E-06
0.250	2.261E-06	6.835E-05	6.828E-05	6.850E-05	4.596E-06	3.814E-06
0.375	3.429E-06	6.884E-05	6.875E-05	6.903E-05	7.046E-06	5.912E-06
0.500	4.619E-06	6.774E-05	6.763E-05	6.798E-05	9.409E-06	7.822E-06
0.625	5.832E-06	6.975E-05	6.966E-05	7.003E-05	1.194E-05	9.929E-06
0.750	7.070E-06	7.039E-05	7.034E-05	7.070E-05	1.456E-05	1.207E-05
0.875	8.330E-06	7.106E-05	7.098E-05	7.144E-05	1.727E-05	1.429E-05
0.1	9.632E-06	7.135E-05	7.124E-05	7.176E-05	2.014E-05	1.663E-05

The hybrid method was utilised for problem (4.1) with parameters $\alpha = 25$ and $\beta = \frac{1}{90}$. A comparative analysis was performed between the hybrid scheme and the other aforementioned methods, utilising the established exact solution as a benchmark to calculate the mean absolute errors across 10,000 sample paths. Error statistics are summarised in Table 1. Employing $N = 32$ sample paths for the Euler-Maruyama, Milstein, and stochastic Runge-Kutta (Platen) methods, the hybrid method exhibits enhanced performance regarding mean absolute error. The block-pulse and hat-function methods yield slightly lower mean absolute errors compared to the hybrid algorithm, but the discrepancies are minimal. Figure 2 displays the mean approximate solution alongside fifteen individual solution trajectories that correspond to fifteen unique Brownian motion sample paths.

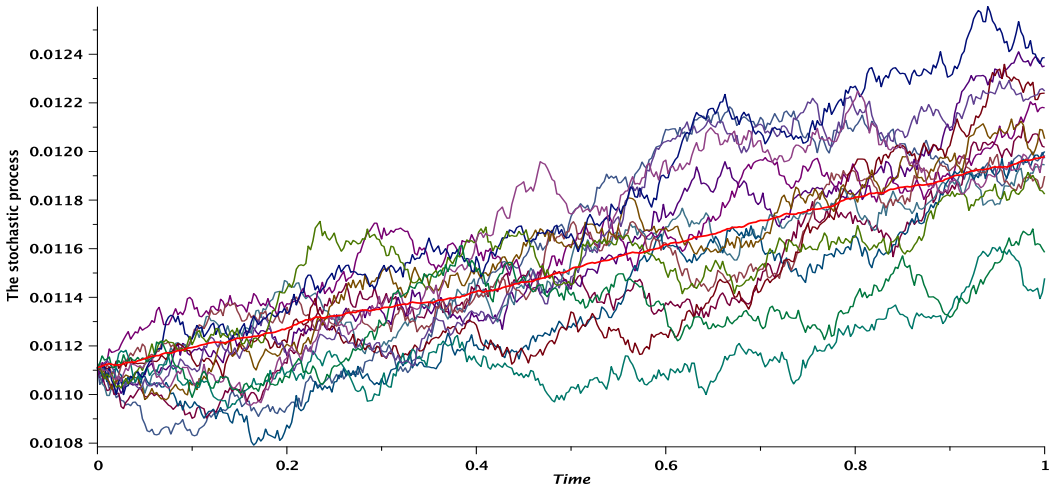

Figure 2: Plot of 15 sample paths and the average of 10000 paths (Mean) of Example 4.1.

Example 4.2 *Consider the stochastic process, Y_t satisfying the subsequent nonlinear SDE [40]:*

$$dY_t = -\frac{1}{\alpha^2} Y_t(1 - {Y_t}^2)dt + \frac{1}{\alpha}(1 - {Y_t}^2)dB(t), \qquad t \in [0, 1], \tag{4.3}$$

where $Y(0) = \beta < 1$, and the exact stochastic process is

$$Y_t \;=\; \tanh\Big(\operatorname{arctanh}(\beta) \;+\; \tfrac{1}{\alpha}\, B_t\Big). \tag{4.4}$$

Table 2: The average absolute error calculated across 10,000 sample paths for Example 4.2.

Time	Present Method $P = 8$	Euler-Maruyama $N = 64$ [13]	Milstein $N = 64$ [7]	Platen $N = 64$ [22]	Block Pulse $N = 8$ [3]	Hat Functions $N = 8$ [11]
0.125	3.891E-06	4.072E-03	4.072E-03	3.636E-03	5.663E-06	4.319E-06
0.250	5.748E-06	3.958E-03	3.958E-03	3.535E-03	9.264E-06	7.917E-06
0.375	9.211E-06	3.992E-03	3.992E-03	3.565E-03	2.033E-05	1.364E-05
0.500	1.308E-05	3.985E-03	3.985E-03	3.560E-03	2.321E-05	2.059E-05
0.625	1.737E-05	3.983E-03	3.983E-03	3.558E-03	2.559E-05	3.477E-05
0.750	2.216E-05	3.917E-03	3.917E-03	3.500E-03	3.643E-05	3.933E-05
0.875	2.724E-05	3.971E-03	3.971E-03	3.549E-03	3.516E-05	4.387E-05
1	3.297E-05	4.033E-03	4.033E-03	3.604E-03	3.518E-05	4.343E-05

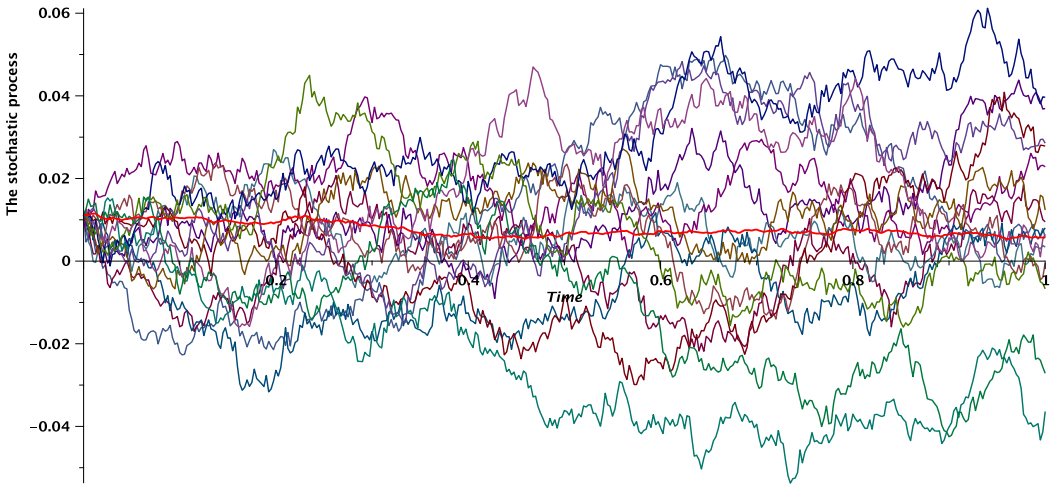

Figure 3: Plot of 15 sample paths and the average of 10000 paths (Mean) of Example 4.2.

The hybrid method was employed for problem (4.2) with parameters $\alpha = 25$ and $\beta = \frac{1}{90}$. A comparative analysis was conducted between the hybrid scheme and the previously mentioned methods, using the established exact solution as a benchmark to compute the mean absolute errors across 10,000 sample paths. Error statistics are consolidated in Table 2. Utilising $N = 64$ sample paths for the Euler-Maruyama, Milstein, and stochastic Runge-Kutta (Platen) methods, the hybrid approach demonstrates superior performance in terms of mean absolute error. The block-pulse and hat-function methods produce marginally lower mean absolute errors than the hybrid algorithm, though the differences are negligible. Figure 3 illustrates the mean approximate solution in conjunction with fifteen distinct solution trajectories corresponding to fifteen unique Brownian motion sample paths.

Example 4.3 *Define the process Y_t through the subsequent nonlinear SDE [43]:*

$$dY_t = -\frac{1}{\alpha^2}\sin(Y_t)\cos^3(Y_t) + \frac{1}{\alpha}\cos^2(Y_t)dB(t), \qquad t \in [0,1], \tag{4.5}$$

For $Y(0) = \beta$, the exact stochastic process is

$$Y_t \;=\; \arctan\Big(\tan(\beta) + \tfrac{1}{\alpha}\,B(t)\Big).$$

Table 3: The average absolute error calculated across 10,000 sample paths for Example 4.3.

Time	Present Method $P = 8$	Euler-Maruyama $N = 64$ [13]	Milstein $N = 64$ [7]	Platen $N = 64$ [22]	Block Pulse $N = 8$ [3]	Hat Functions $N = 8$ [11]
0.125	2.290E-06	3.394E-03	3.394E-03	3.393E-03	4.078E-06	3.112E-06
0.250	3.450E-06	3.299E-03	3.299E-03	3.299E-03	8.262E-06	5.514E-06
0.375	5.504E-06	3.327E-03	3.327E-03	3.327E-03	1.413E-05	9.859E-06
0.500	7.784E-06	3.321E-03	3.321E-03	3.321E-03	1.971E-05	1.306E-05
0.625	1.030E-05	3.320E-03	3.320E-03	3.320E-03	2.685E-05	1.828E-05
0.750	1.310E-05	3.265E-03	3.265E-03	3.265E-03	3.416E-05	2.260E-05
0.875	1.607E-05	3.311E-03	3.311E-03	3.311E-03	4.257E-05	2.865E-05
1	1.941E-05	3.362E-03	3.362E-03	3.362E-03	5.119E-05	3.368E-05

For problem (4.3), the hybrid method was employed, utilising parameters $\alpha = 30$ and $\beta = \frac{1}{100}$. A comparative analysis was conducted to compute the average absolute errors across 10,000 sample paths

between the hybrid scheme and the previously mentioned methods. The definitive solution that was established served as the standard for this analysis. The error statistics are compiled and displayed in Table 3. The hybrid approach exhibits enhanced performance regarding mean absolute error when compared with the Euler-Maruyama, Milstein, and stochastic Runge-Kutta (Platen) methods. This is due to the utilisation of $N = 64$ sample paths. The block-pulse and hat-function methods yield mean absolute errors that are slightly lower than those generated by the hybrid algorithm; nonetheless, the discrepancies between the two methods are negligible. Figure 3 illustrates the average approximate solution alongside fifteen unique solution trajectories corresponding to fifteen different Brownian motion sample paths.

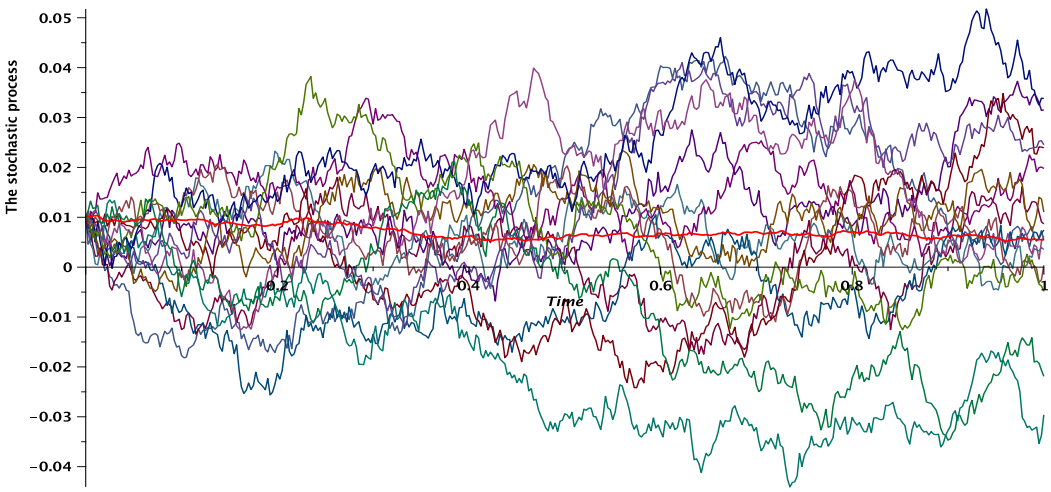

Figure 4: Plot of 15 sample paths and the average of 10000 paths (Mean) of Example 4.3.

Example 4.4 *The governing equation for Y_t is the nonlinear SDE presented here [33]:*

$$dY_t = -\frac{1}{\alpha^2}\tanh(Y_t)sech^2(Y_t) + \frac{1}{\alpha}sech(Y_t)dB(t), \qquad t \in [0,1], \tag{4.6}$$

For $Y(0) = \beta$, the exact stochastic process is

$$Y_t = \operatorname{arcsinh}(\frac{1}{\alpha}B(t) + \sinh(\beta)).$$

Table 4: The average absolute error calculated across 10,000 sample paths for Example 4.4.

Time	Present Method $P = 8$	Euler-Maruyama $N = 64$ [13]	Milstein $N = 64$ [7]	Platen $N = 64$ [22]	Block Pulse $N = 8$ [3]	Hat Functions $N = 8$ [11]
0.125	2.804E-06	3.636E-03	3.636E-03	3.636E-03	4.078E-06	2.732E-06
0.250	4.207E-06	3.535E-03	3.535E-03	3.535E-03	8.262E-06	5.287E-06
0.375	6.719E-06	3.566E-03	3.565E-03	3.565E-03	1.413E-05	9.149E-06
0.500	9.513E-06	3.560E-03	3.560E-03	3.560E-03	1.971E-05	1.256E-05
0.625	1.260E-05	3.558E-03	3.558E-03	3.558E-03	2.685E-05	1.720E-05
0.750	1.604E-05	3.500E-03	3.500E-03	3.500E-03	3.416E-05	2.160E-05
0.875	1.968E-05	3.549E-03	3.549E-03	3.549E-03	4.257E-05	2.702E-05
1	2.378E-05	3.604E-03	3.604E-03	3.604E-03	5.119E-05	3.212E-05

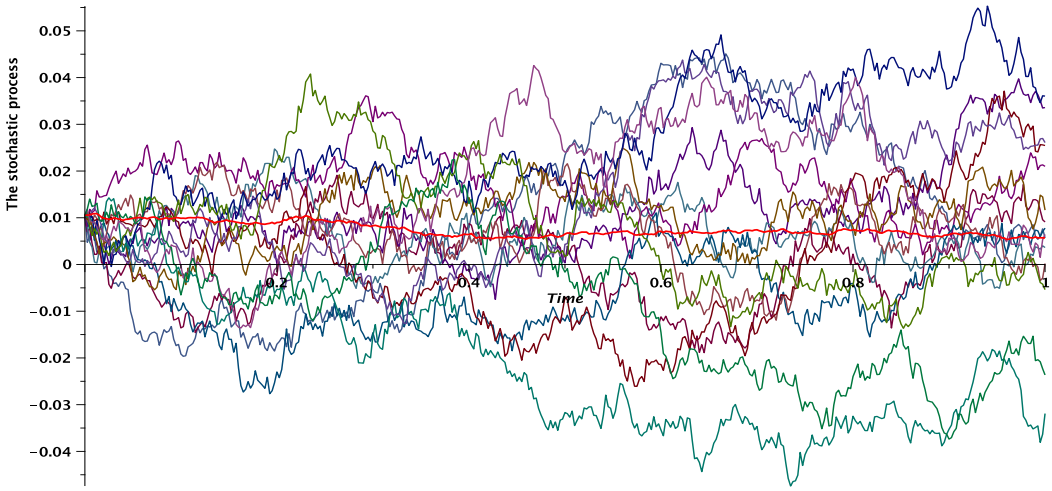

Figure 5: Plot of 15 sample paths and the average of 10000 paths (Mean) of Example 4.4.

The hybrid method was utilised for problem (4.4) with parameters $\alpha = 28$ and $\beta = \frac{1}{95}$. A comparative analysis was performed between the hybrid scheme and the aforementioned methods, utilising the established exact solution as a benchmark to calculate the average absolute errors across 10,000 sample paths. Error statistics have been compiled in Table 4. Employing $N = 64$ sample paths for the Euler-Maruyama, Milstein, and stochastic Runge-Kutta (Platen) methods, the hybrid approach exhibits enhanced performance regarding mean absolute error. The block-pulse and hat-function methods yield slightly lower mean absolute errors compared to the hybrid algorithm, although the discrepancies are minimal. Figure 4 depicts the average approximate solution alongside fifteen distinct solution trajectories associated with fifteen unique Brownian motion sample paths.

5. Conclusions

This work adopts a novel hybrid method for solving nonlinear SDEs numerically. This method is based on companion Chebyshev polynomials and classical deterministic RK4 methods. Chebyshev polynomials have been used to approximate each Brownian sample path over the given time horizon. This process reduces the considered nonlinear SDEs into a family of deterministic nonlinear ODEs with polynomial forcing terms. We aim to take advantage of the exponential convergence and global approximation capabilities of Chebyshev spectral methods while maintaining simplicity and stability. Meanwhile, regarding the local adaptability of traditional RK4 methods.

Using 10,000 sample paths of Brownian motion, each consisting of N points, we give a complete, comprehensive, and uniformly applied each realisation across five numerical methods, including the Euler-Maruyama, Milstein, Stochastic Runge-Kutta (Platen), block-pulse, and hat-function methods. Extensive numerical experiments on various test cases have shown that the hybrid method attains significantly lower absolute average errors compared with other methods. In fact, the hybrid method provides a flexible and effective instrument for professionals pursuing accurate simulations of nonlinear SDEs.

Our numerical results indicate that the hybrid method encompasses classical piecewise-continuous bases as specific instances and provides comparable or enhanced accuracy and robustness across a wide range of test problems. Its capacity to modify the polynomial degree offers a methodical approach to exchanging local support for global spectral resolution. Future efforts will concentrate on adaptive degree selection informed by forward error estimators, extensions to fractional stochastic differential equations, and applications to high-dimensional, time-dependent systems. We expect this adaptable framework to be a significant resource for researchers and engineers addressing intricate deterministic and stochastic modelling issues.

Acknowledgments

We think the referee by your suggestions.

References

1. Abdul-Wahhab, R. D., Eisa, M. M., and Khalaf, S. L. *The study of stability analysis of the ebola virus via fractional model*. Partial Differ. Equations Appl. Math. 11 100792 (2024).
2. Arnold, L. *Stochastic differential equations: theory and applications*. Springer (1974).
3. Asgari, M. and Shekarabi, F. *Numerical solution of nonlinear stochastic differential equations using the block pulse operational matrices*. Math. Sci. (Springer) 7(1) 47 (2013).
4. Barikbin, M., Vahidi, A., Damercheli, T., and Babolian, E. *An iterative shifted chebyshev method for nonlinear stochastic itÃ´-volterra integral equations*. J. Comput. Appl. Math. 378 112912 (2020).
5. Boyd, J. P. *Chebyshev and Fourier Spectral Methods*. Dover Publications, Mineola, New York, 2nd revised edition (2001).
6. Bressloff, P. C. *Stochastic processes in cell biology*, volume 41. Springer (2014).
7. Burrage, K., Lenane, I., and Lythe, G. *Numerical methods for secondâ-order stochastic differential equations*. SIAM J. Sci. Comput. 29(1) 245–264 (2007).
8. Dareiotis, K. and Leahy, J.-M. *Finite difference schemes for linear stochastic integro-differential equations*. Stochastic Process. Appl. 126(10) 3202–3234 (2016).
9. Gao, J., Liang, H., and Ma, S. *Strong convergence of the semi-implicit euler method for nonlinear stochastic volterra integral equations with constant delay*. Appl. Math. Comput. 348 385–398 (2019).
10. Guo, Q., Mao, X., and Yue, R. *The truncated eulerâ-maruyama method for stochastic differential delay equations*. Numer. Algorithms 78(2) 599–624 (2017).
11. Heydari, M., Hooshmandasl, M., Maalek Ghaini, F., and Cattani, C. *A computational method for solving stochastic itÃ´-volterra integral equations based on stochastic operational matrix for generalized hat basis functions*. J. Comput. Phys. 270 402–415 (2014).
12. Heydari, M. H., Hooshmandasl, M. R., Shakiba, A., and Cattani, C. *Legendre wavelets galerkin method for solving nonlinear stochastic integral equations*. Nonlinear Dynam. 85(2) 1185–1202 (2016).
13. Higham, D. J. *An algorithmic introduction to numerical simulation of stochastic differential equations*. SIAM Rev. 43(3) 525–546 (2001).
14. Karatzas, I. and Shreve, S. E. *Brownian Motion and Stochastic Calculus*. Springer, New York, 2nd edition (1991).
15. Khalaf, S. L. and Kadhim, M. S. *Design of optimal control for the in-host tuberculosis fractional model*. Iraqi J. Sci. (6401–6412) (2023).
16. Khalaf, S. L., Kassid, K. K., and Khudair, A. R. *A numerical method for solving quadratic fractional optimal control problems*. Results Control Optim. 13 100330 (2023).
17. Khalil, W. I. and Khudair, A. R. *Mathematical analysis of covid-19 dynamics in iraq utilising empirical data*. Results Control Optim. 18 100528 (2025).
18. Khodabin, M., Maleknejad, K., Rostami, M., and Nouri, M. *Interpolation solution in generalized stochastic exponential population growth model*. Appl. Math. Modell. 36(3) 1023–1033 (2012).
19. Khudair, A. R. *Reliability of adomian decomposition method for high order nonlinear differential equations*. Appl. Math. Sci. 7 2735–2743 (2013).
20. Khudair, A. R., Ameen, A. A., and Khalaf, S. L. *Mean square solutions of second-order random differential equations by using adomian decomposition method*. Appl. Math. Sci. 5(49–52) 2521–2535 (2011).
21. Khudair, A. R., Ameen, A. A., and Khalaf, S. L. *Mean square solutions of second-order random differential equations by using variational iteration method*. Appl. Math. Sci. 5(49–52) 2505–2519 (2011).
22. Kloeden, P. E. and Platen, E. *Numerical Solution of Stochastic Differential Equations*. Springer Berlin Heidelberg (1992).
23. Kloeden, P. E., Platen, E., Kloeden, P. E., and Platen, E. *Stochastic differential equations*. Springer (1992).
24. Kuznetsov, D. F. *A comparative analysis of efficiency of using the legendre polynomials and trigonometric functions for the numerical solution of ito stochastic differential equations*. Comput. Math. Math. Phys. 59(8) 1236–1250 (2019).
25. Mahdi, N. and Khudair, A. *Some delta q-fractional linear dynamic equations and a generalized delta q-mittag-leffler function*. Comput. Methods Differ. Equ. (Online First) (2023).
26. Mahdi, N. K. and Khudair, A. R. *An analytical method for q-fractional dynamical equations on time scales*. Partial Differ. Equations Appl. Math. 8 100585 (2023).

27. Mahdi, N. K. and Khudair, A. R. *The delta q-fractional gronwall inequality on time scale.* Results Control Optim. 12 100247 (2023).

28. Mahdi, N. K. and Khudair, A. R. *Linear fractional dynamic equations: Hyers-ulam stability analysis on time scale.* Results Control Optim. 14 100347 (2024).

29. Mahdi, N. K. and Khudair, A. R. *Toward stability investigation of fractional dynamical systems on time scale.* Turk. World Math. Soc. J. Appl. Eng. Math. 14(4) 1495–1513 (2024).

30. Mahdi, N. K. and Khudair, A. R. *Some analytical results on the δ-fractional dynamic equations.* Turk. World Math. Soc. J. Appl. Eng. Math. 15(3) 577–589 (2025).

31. Miller, R. K. *On volterraâ-s population equation.* SIAM J. Appl. Math. 14(3) 446–452 (1966).

32. Mirzaee, F. and Hadadiyan, E. *A collocation technique for solving nonlinear stochastic itÃ´â-volterra integral equations.* Appl. Math. Comput. 247 1011–1020 (2014).

33. Mirzaee, F. and Hamzeh, A. *A computational method for solving nonlinear stochastic volterra integral equations.* J. Comput. Appl. Math. 306 166–178 (2016).

34. Mirzaee, F. and Samadyar, N. *Application of orthonormal bernstein polynomials to construct a efficient scheme for solving fractional stochastic integro-differential equation.* Optik 132 262–273 (2017).

35. Mirzaee, F. and Samadyar, N. *On the numerical solution of fractional stochastic integro-differential equations via meshless discrete collocation method based on radial basis functions.* Eng. Anal. Bound. Elem. 100 246–255 (2019).

36. Mirzaee, F., Samadyar, N., and Hoseini, S. F. *Euler polynomial solutions of nonlinear stochastic itÃ´â-volterra integral equations.* J. Comput. Appl. Math. 330 574–585 (2018).

37. Mohammed, J. K. and Khudair, A. R. *A novel numerical method for solving optimal control problems using fourth-degree hat functions.* Partial Differ. Equations Appl. Math. 7 100507 (2023).

38. Mohammed, J. K. and Khudair, A. R. *Solving nonlinear stochastic differential equations via fourth-degree hat functions.* Results Control Optim. 12 100291 (2023).

39. Mohammed, J. K. and Khudair, A. R. *Solving volterra integral equations via fourth-degree hat functions.* Partial Differ. Equations Appl. Math. 7 100494 (2023).

40. Øksendal, B. *Stochastic Differential Equations: An Introduction with Applications.* Springer, Berlin, Heidelberg, 6th edition (2003).

41. Padgett, W. and Tsokos, C. *A stochastic model for chemotherapy: computer simulation.* Math. Biosci. 9 119–133 (1970).

42. Shen, J., Tang, T., and Wang, L.-L. *Spectral Methods: Algorithms, Analysis and Applications.* Springer Berlin Heidelberg (2011).

43. Shiralashetti, S. and Lamani, L. *Fibonacci wavelet based numerical method for the solution of nonlinear Stratonovich Volterra integral equations.* Scientific African 10 e00594 (2020).

44. Soong, T. T. and Bogdanoff, J. L. *Random differential equations in science and engineering.* J. Appl. Mech. 41(4) 1148–1148 (1974).

45. Susanto, H., Kevrekidis, P., Abdullaev, F., and Malomed, B. A. *Symmetry breaking, coupling management, and localized modes in dual-core discrete nonlinear-schrÃ¶dinger lattices.* J. Comput. Appl. Math. 235(13) 3883–3888 (2011).

46. Tocino, A. and Ardanuy, R. *Rungeâ-kutta methods for numerical solution of stochastic differential equations.* J. Comput. Appl. Math. 138(2) 219–241 (2002).

47. Trefethen, L. N. *Spectral Methods in MATLAB.* Society for Industrial and Applied Mathematics (2000).

Ayad R. Khudair,

Department of Mathematics,

University of Basrah,

Iraq.

E-mail address: ayadayad1970@yahoo.com